Theor Chem Acc (2012) 131:1097
DOI 10.1007/s00214-012-1097-y

REGULAR ARTICLE

Imperfect periodicity and systematic changes of some structural features along linear polymers: the case of rod-like boron/nitrogen nanostructures

Eva Simon · Paul G. Mezey

Received: 11 October 2011 / Accepted: 1 November 2011 / Published online: 10 February 2012

Abstract Systematic changes of structural features along polymers are often manifested in deviations from periodicity, having important roles in biopolymers, as well as in simpler systems, where these very deviations are easier to recognize and analyze. Some approximately periodic rod-like structures, called nanoneedles show special, systematic deviations from periodicity. According to our theoretical study, there is a special bonding pattern, involving stronger bonds along the nanoneedle than within the formal rings of layers across the nanoneedle, and there is a monotonic change of some bond lengths from one end to the other along these thin rods. In a series of geometry-optimized Hydrogen-capped boron/nitrogen nanoneedles, regarded as potential semi-rigid building elements of nanostructures, the lengths of bonds roughly parallel with the axes change strictly monotonically from the B–H ends to the N–H ends. The B3LYP/6-31G(d, p) level of density-functional theory computational methods have been used for this $H_3(B_3N_3)_nH_3$ ($n = 2$–10) series of nanoneedles, and an electron density shape description has been applied using a series of molecular isodensity contours. Longer bonds in formally identical structural elements usually indicate weaker linkages. Consequently, such nanoneedles may serve as special structural elements in nanotechnology where various levels of local deformability are required. Additional computational tests on rigidity have been performed: the geometries of these boron nitride nanoneedles were subjected to small modifications and the energy requirements of these deformations were calculated.

Keywords Nanoneedle · DFT · Electron density · Nanotechnology

1 Introduction

Studies on one-dimensional polymers often must address the problem of imperfect periodicity. Such a problem is typical in many biochemically important polymers since most one-dimensional biopolymers owe a major part of their functionality and diversity to the fact that they show only quasi-periodicity. A typical case is the structure of DNA, and practically, all natural peptides and proteins are also only quasi-periodic. Perfect periodicity is a great technical advantage in computational molecular modeling, as recognized in early quantum chemistry studies on biopolymers [1]; however, the lack of exact periodicity renders most of the simpler modeling methods inadequate. Among the more advanced methods used to overcome the lack of perfect periodicity, the works of Akira Imamura and many of his colleagues are especially noteworthy; the so-called elongation method has been shown to provide efficient solutions to some of the related problems [2–7].

The deviations from periodicity may be severe, for example, in one-dimensional polymers with diverse

Dedicated to Professor Akira Imamura on the occasion of his 77th birthday; this article was intended for publication in the Imamura Festschrift Issue of TCA, volume 130, numbers 4–6, December 2011, but was not yet in final form at the time of that issue's completion.

E. Simon · P. G. Mezey (✉)
Scientific Modeling and Simulation Laboratory (SMSL), Department of Chemistry and Department of Physics and Physical Oceanography, Memorial University of Newfoundland, 283 Prince Philip Dr., St. John's, NF A1B3X7, Canada
e-mail: paul.mezey@gmail.com

P. G. Mezey
Institute of Chemistry, Eötvös University, Budapest, Hungary

monomeric units assembled randomly, where no bonding pattern along the chain shows regular repetition. In some other cases, the lack of perfect periodicity may be less serious, for example, in most peptides and proteins, where at least some bonding patterns are repeated regularly along the one-dimensional chain. In these systems, the deviation from periodicity is caused only by the differences in some side chains attached to a main molecular chain that by itself appears periodic.

One may, however, consider the even simpler cases of very small deviations from periodicity, where the chemical composition of the monomeric units is formally the same along the chain, only some minor geometrical differences are found between the monomeric units along the chain. These small differences result in the imperfectness of periodicity. For example, this is the case in model systems where the lack of perfect periodicity originates from structural differences only at the two ends of the polymer of rather limited length. Otherwise, the monomeric units are formally the same along the chain. Nevertheless, these special "end effects" can produce some minor changes through interactions with neighboring monomeric units.

In this study, we shall consider such a "nearly perfectly periodic" case of non-periodicity in a non-biopolymer example caused only by "end effects," where the non-periodicity is manifested merely in the slight variations in the bond lengths values. Otherwise, the chemical formulas and even the connectivities of the monomeric units are exactly the same, except at the two ends of the finite polymer.

In such cases, one may expect some interesting regularities in the manifestation of the slight non-periodicity, since as the distance from the two ends of the polymer increases along the chain, the role of the "end effect" and the roles of further induced "near end effects" are expected to diminish by distance along the chain.

One further consideration is the interactions of various units, which are formally far apart along the chain, but because of bending of the polymer, these monomeric units may end up close to one another. Consequently, their interactions may become far more significant than it would be expected based simply on the large differences in their sequence numbers along the chain. Of course, such occurrences are obscuring whatever regularities may exist otherwise for polymers without such bending, that is, when only the position of the monomeric units along the chain matters.

Therefore, polymers that do not bend over themselves, that is, polymers that are rod-like, provide the simplest models where the regularities appearing in the slight non-periodicity caused by "end effects" can be studied without obscuring interactions. Of course, rod-like structures are of special interest when one considers their potential role in nanotechnology as structural elements, such as spacer rods keeping parts at some distance. However, they are also interesting theoretically, since their conformational variations are typically very limited, representing special cases in both conformational potential surface studies [8, 9] and molecular shape analysis [10].

Along some narrow, rod-like structures, with bonds generated by the same atom pair, one does not expect significant variations in bonding patterns. However, the results of this study show that uniform stepwise build-up of certain nanoneedles can lead to systematic variations in bonding along the axes of these needles, which persists even for the longer structures studied. In the past decades, considerable interest has developed in various nanostructure systems as potential building blocks in nanotechnology. In particular, the boron nitride (BN) structures [11] have been assumed to have special importance because of their potentially useful electronic, mechanical, and optical properties. In early studies, various electronic properties of two-dimensional hexagonal boron nitride clusters [12, 13] were studied using the semi-empirical LCAO methods, such as the extended Hückel (EXH) [14], the iterative extended Hückel (IEXH) [15], and the intermediate neglect of differential overlap (INDO) [16]. These results have been compared with more advanced SCF ab initio calculations and experimental results. Electronic and structural properties of BN systems were also studied using the ab initio pseudopotential total energy method [17]. Recent theoretical studies have been performed on single- and multi-wall BN nanotubes [18], SWBNNT–MWBNNT, based on ab initio pseudopontetial local-density-functional (LDA) and quasi-particle calculations. Other theoretically studied structures [19], borazine-fused cyclacenes, were optimized using RHF/6-31G(d) and B3LYP/6-31G(d) levels of theory.

Experimentally studied SWBNNT and MWBNNT have also been reported where a variety of methods were used; for instance, scanning tunneling spectroscopy (STS) [20, 21] and high-resolution transmission electron microscopy (HRTEM) [22, 23] have been employed. Various BN nanotubes have been already synthesized applying arc discharge techniques [24, 25].

Moreover, optical properties of the SWBN and MWBN nanotubes have been experimentally studied [26, 27] by means of optical absorption spectroscopy. Ab initio calculations were also performed by studying the optical absorption spectra of small-diameter boron nitride nanotubes [28, 29].

The geometry of a family of much more tightly packed carbon or nitrogen nanotubes with narrow, inaccessible interior, called nanoneedles [30, 31], has also been investigated. Analogous structures with nitrogen and boron atoms instead of carbon atoms are potentially providing alternatives to rigid spacer rods. A related sequence of studies involved spiral arrangement of B and N atoms, analogous to hexahelicene [32–34].

In this article, we present a theoretical study of a series of energetically favored boron/nitrogen nanoneedles (BNNNs), $H_3(B_3N_3)_nH_3$, $n = 2$–10, using DFT quantum mechanical computational method at the B3LYP/6-31G(d, p) level, where both the internal regions and the peripheral regions of the nanoneedles show characteristic patterns. For the analysis of these nanoneedles patterns, electron density analysis is applied using a series of molecular isodensity contours (MIDCO's). Earlier studies also using the B3LYP/6-31G(d) methodology on boron-fused cyclacenes [9], as well as comparative studies on BN helicenes have provided justification for the methodology [22–24]. In order to elucidate the systematic bond length variations along the needles and their relation to the changes in rigidity along the needles, actual geometry modifications have also been introduced, where the energy changes provide direct measures for rigidity.

2 Computational methodology

The Gaussian 03 software package [35] is used for geometry optimization and vibrational frequency calculations. The special geometrical features and the energetic stability of the series of boron/nitrogen nanoneedles have been calculated at the B3LYP level of density-functional theory (DFT) using the 6-31G(d, p) basis set. The series of molecular isodensity contours (MIDCO's) for various density thresholds are presented using the MOLEKEL 4.3 molecular visualization program [36].

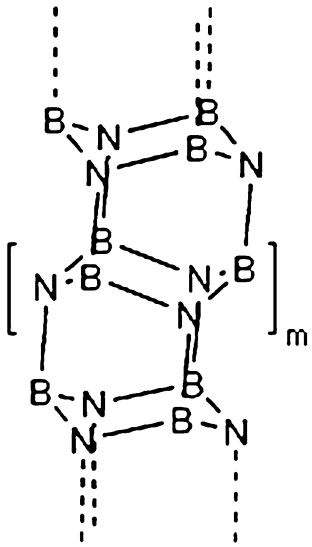

Fig. 1 Geometric pattern of central parts of all nanoneedles $H_3(B_3N_3)_nH_3$ with $n \geq m + 2$ B_3N_3 layers

3 Results and discussion

Using initial structures patterned by the analogous carbon or nitrogen nanoneedles of earlier studies [30, 31], energy minima were found for a series of boron/nitrogen nanoneedles formed by B_3N_3 unit layers and three hydrogen atoms on both ends of the needles (Fig. 1).

Four energy optimized conformers of each type of the compounds, $H_3(B_3N_3)_nH_3$, $n = 2$–10, were obtained, where the N–H bond's axial (a) or equatorial (e) alignment, in four possible combinations, is shown in Fig. 2 describing the N-terminal regions of the BNNNs. The geometry of the other end where the B–H bonds are located does not show conformational variations and is nearly the same in any of the structures. All four conformations of each length n have been optimized and are found to be proper energy minima with all real vibrational frequencies.

The two lowest energy conformations, except $n = 2$, are the (aea)-BNNN and (eae)-BNNN structures, where the second one is the most stable and this can be observed as a general trend if the length of the needle is increased by adding B_3N_3 unit layers.

Relative energies of the conformers for each n are represented in Fig. 3, where the reference (eae) conformer has the lowest energy. The (eae) conformer is more stable than (aea) by an average of 1.0 kJ/mol, it is lower than (aaa) conformer by 22.6 kJ/mol and lower than (eee) by 32.1 kJ/mol. Figure 3 and the calculated data already show that the lone-pair repulsion has an important influence on the relative energy.

The bonding pattern of the structures shows that the bond lengths between layers are always shorter than those within layers; consequently, the strength of the bond is stronger between layers than it is within layers. This is a strong indication that long needles are indeed feasible. For instance, the bond lengths of $H_3(B_3N_3)_6H_3$ are 1.435–1.474 Å between layers and 1.471–1.526 Å within rings, shown in Figs. 4 and 5, respectively. We have also observed that the lengths of the axial B–N bonds are decreasing monotonically from the N–H end to the B–H end of the

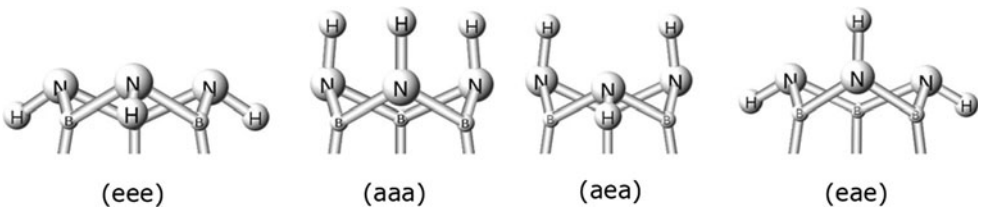

Fig. 2 The (*eee*), (*aaa*), (*aea*), and (*eae*) conformations of the boron/nitrogen nanoneedles

molecules, whereas the bond lengths within each layer are nearly constant, as shown in Fig. 5. This finding provides suggestions that stretching of these rods is apparently somewhat easier near the N–H ends of the rods, and the rods are more rigid closer to the B–H ends. The systematic bond length variations suggest "tapered" rigidity levels along the rods, which might be a useful property in the construction of nanodevices: nanorods with some control on rigidity. Actual deformations of the optimal geometries and direct tests on the associated energy variations (vide infra) provide the connections between bond length variations and actual local rigidity of these structures. Note that, analogous rod-like GaN structures have been studied earlier [37–40], where H atoms are attached along the entire length of the rods. According to those studies, the axial bond lengths do not show a systematic, monotonic trend. In the GaN studies, the bond lengths within the six-membered rings forming subsequent levels of the rod structures do show systematic changes; this latter trend of bond length variations from level-to-level of within ring bonds is also evident for the BN nanoneedles of the present study. However, the primary focus of our observation, on the strictly monotonic bond length changes parallel to the needle axis is apparently a novel finding.

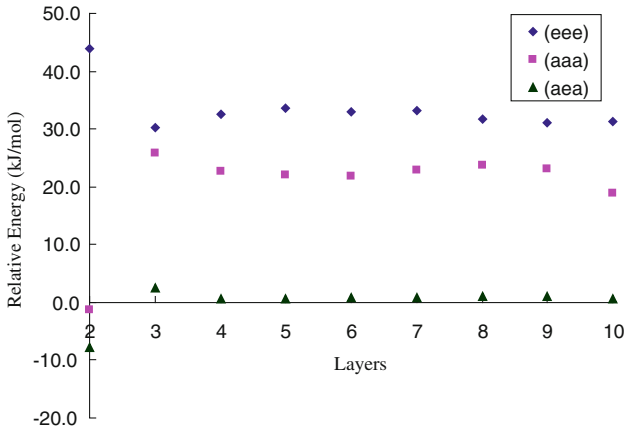

Fig. 3 Relative energy (kJ/mol) of the (*eee*) (*aaa*) (*aea*) conformers of each length *n*, as compared to the energy of the usually most stable (*eae*) conformer

As indicated in the variation of terminal bond length differences with *n*, shown in Table 2 for each of the four nanoneedle series (eee), (aaa), (aea), and (eae), the extent of this tapered bond length variation along the needles is strongly dependent on the conformation of the N–H terminal of the needles. For the (aaa) series, the difference in

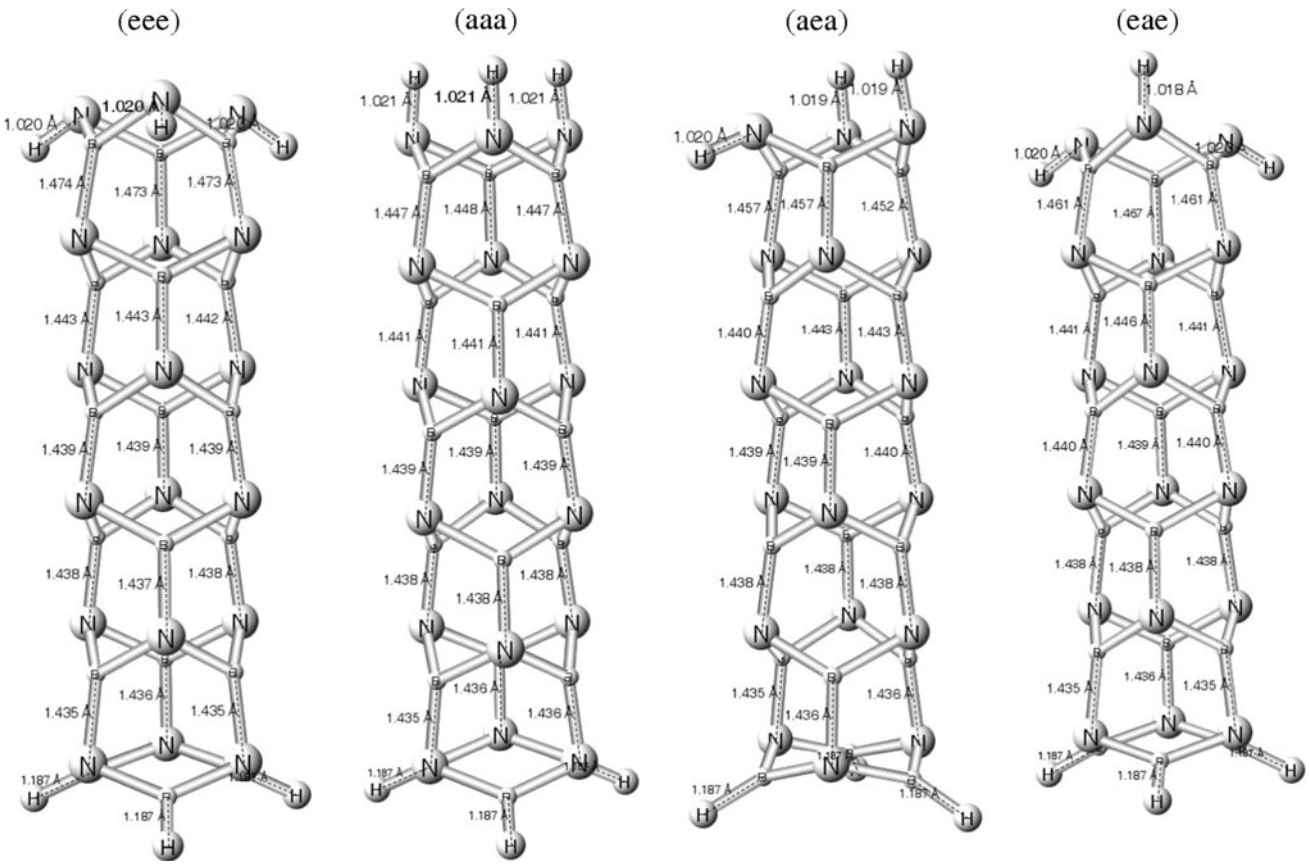

Fig. 4 Bond lengths between layers of the (*eee*), (*aaa*), (*aea*), and (*eae*) $H_3(B_3N_3)_6H_3$ conformers

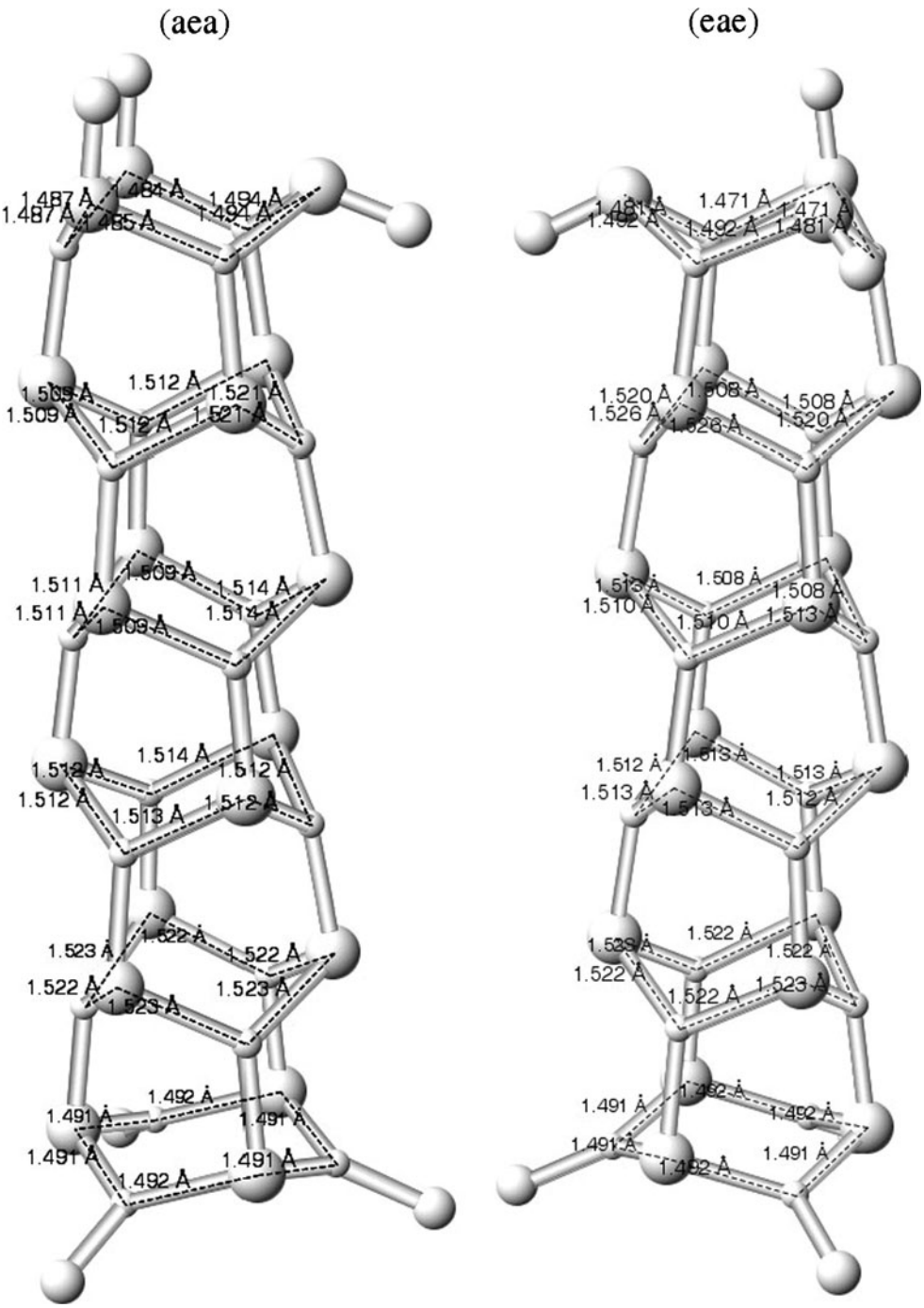

Fig. 5 Bond lengths within layers of the (*aea*) and (*eae*) $H_3(B_3N_3)_6H_3$ conformers

the terminal bond lengths stabilizes at 0.013 Å as *n* increases; this is the minimum range for tapering when compared to the other three sequences. By contrast, sequence (eee) shows the maximum range of tapering, the difference between terminal bond lengths quickly converges to 0.038 Å as *n* increases. Apparently, the axial orientation of the lone pairs at the terminal N–H locations enhances this tapering effect.

In the other two sequences, (aea) and (eae), the terminal N–H groups are no longer equivalent, nevertheless, the same general tapering effect is clearly manifested, stabilizing at values intermediate between the above two extreme values, as *n* increases.

It is advantageous to study relatively simple systems, such as these BN nanoneedles, as compared, for example, to various biopolymers with complicated and diverse side chains, as well as major deviations from actual periodicity. The structures of the BN nanoneedles are affected by relatively few complex and confusing interactions, and better assumptions can be made for elucidating the cause of

certain features. For example, in more general structures, bond angle and torsion angle influences should also be considered; fortunately, in the present problem, such effects are minor and do not affect the main conclusions about bond length variations. In our case, the only major difference between the four types of BN nanoneedles is the arrangement of the N terminus, where there are only two local features that may matter: the orientation of the N–H bonds and the orientation of the N lone pairs. Even by simple arguments, an equatorial orientation for the N–H bond, that is, an axial orientation of a lone pair on N allows for an effective displacement of electron density from the vicinity of the axial B–N bonds between the first and second layers. This may result in longer B–N bond lengths; therefore, the lone-pair orientation is of major importance, as this is reflected well in the bond length variations. The very monotonicity of bond length changes already strongly suggests that the primary cause must reside at one of the ends of these needles. Having virtually identical B ends, the rather evident choice is the set of lone pairs at the N-terminal: the further away is an axial B–N bond from the N lone pairs, the lesser the influence.

These observations indicate a systematic pattern, valid for all the studied structures, which can become potentially useful if asymmetric local flexibility is required in some nanostructures. Note that in order to avoid any symmetry bias in the actual geometry optimizations no symmetry constrains were employed, and the actual convergence of the optimizations to (almost perfectly) symmetric structures is not an artifact of any initial assumption. Consequently, the symmetry of the optimized structures are considered within the tolerance thresholds of the geometry

Table 1 Bond lengths (Å) between layers of the (eee), (aaa), (aea), and (eae) $H_3(B_3N_3)_6H_3$ conformers

	e	e	e	a	a	a
d_a(N–H end)	1.4733	1.4734	1.4736	1.4476	1.4473	1.4474
	1.4425	1.4427	1.4426	1.4406	1.4406	1.4408
	1.4394	1.4390	1.4390	1.4390	1.4391	1.4388
	1.4376	1.4371	1.4376	1.4378	1.4378	1.4379
d_z(B–H end)	1.4358	1.4351	1.4350	1.4356	1.4357	1.4354
	a	e	a	e	a	e
d_a(N–H end)	1.4568	1.4520	1.4569	1.4609	1.4674	1.4609
	1.4427	1.4399	1.4427	1.4407	1.4462	1.4408
	1.4388	1.4403	1.4390	1.4398	1.4388	1.4398
	1.4379	1.4381	1.4379	1.4377	1.4381	1.4377
d_z(B–H end)	1.4355	1.4356	1.4357	1.4355	1.4356	1.4355

Table 2 The variation of terminal bond lengths (Å) with n for the four nanoneedle series (eee), (aaa), (aea), and (eae)

n	2	3	4	5	6	7	8	9	10
(eee)									
d_a(N–H end)	1.468	1.477	1.476	1.474	1.473	1.473	1.473	1.473	1.472
d_z(B–H end)		1.439	1.438	1.436	1.435	1.435	1.435	1.435	1.434
$D(n) = d_a - d_z$	–	0.038	0.038	0.038	0.038	0.038	0.038	0.038	0.038
(aaa)									
d_a(N–H end)	1.444	1.449	1.449	1.449	1.447	1.448	1.447	1.447	1.447
d_z(B–H end)		1.440	1.437	1.437	1.435	1.435	1.435	1.434	1.434
$D(n) = d_a - d_z$	–	0.009	0.012	0.012	0.012	0.013	0.012	0.013	0.013
(aea)									
maxd_a(N–H end)	1.454	1.460	1.458	1.457	1.456	1.457	1.456	1.456	1.456
maxd_z(B–H end)		1.441	1.439	1.437	1.435	1.435	1.436	1.434	1.435
$D(n) = \max d_a - \max d_z$	–	0.019	0.019	0.020	0.021	0.022	0.020	0.022	0.021
(eae)									
maxd_a(N–H end)	1.461	1.472	1.469	1.468	1.467	1.467	1.467	1.467	1.466
maxd_z(B–H end)		1.443	1.439	1.436	1.435	1.435	1.435	1.434	1.436
$D(n) = \max d_a - \max d_z$	–	0.029	0.030	0.032	0.032	0.032	0.032	0.033	0.030

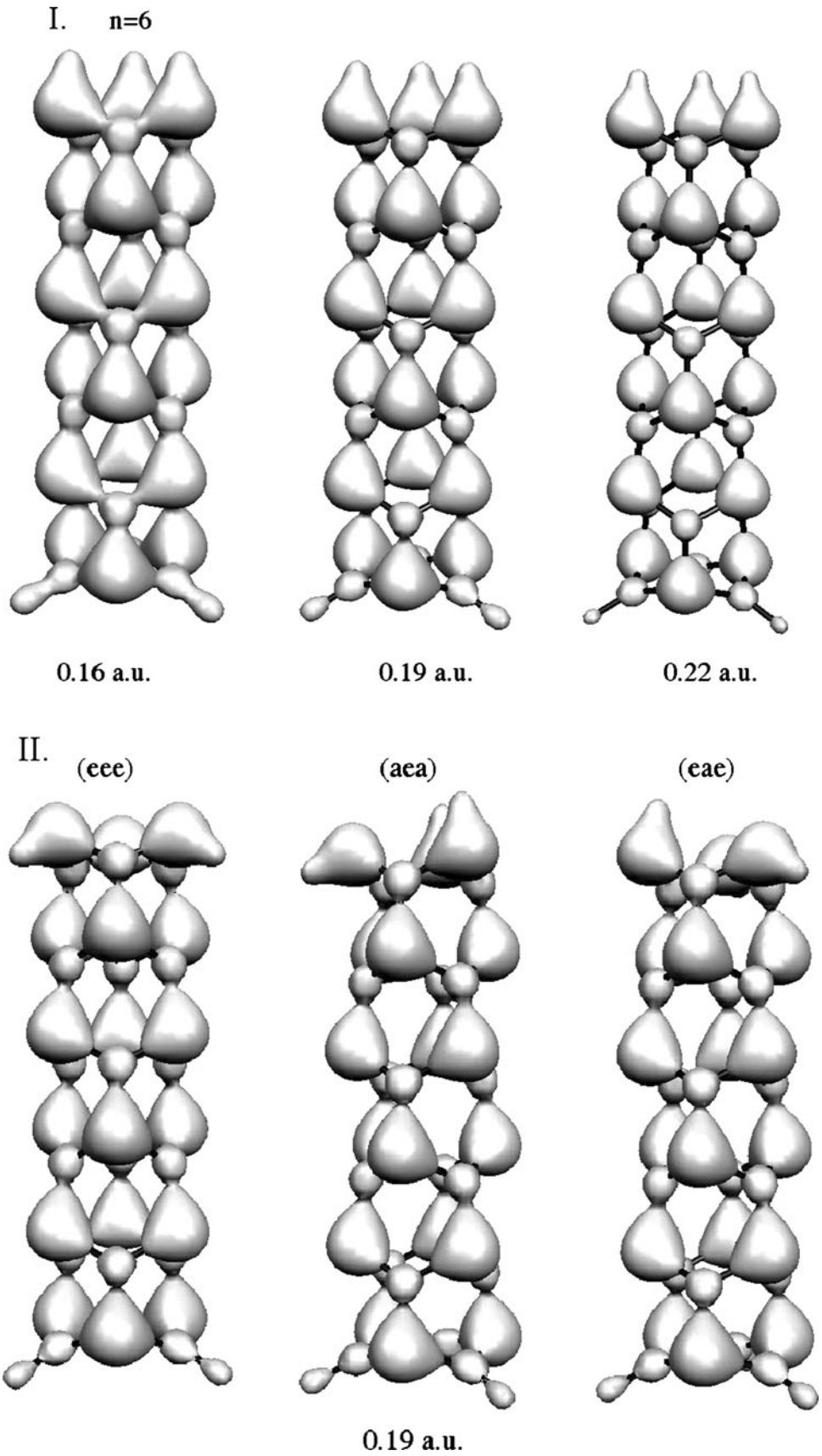

Fig. 6 Isodensity contours of 6 layer—boron/nitrogen nanoneedles: I. (*aaa*) conformer with thresholds of 0.16 a.u., 0.19 a.u., 0.22 a.u., and II. (*eee*), (*aea*), and (*eae*) conformers with threshold of 0.19 a.u

optimization, where bond lengths differences less then 0.001 Angstrom are not regarded as violation of symmetry. To illustrate this aspect, the obtained bond length values are reported for four decimal places in Table 1. In Fig. 4; however, in order to avoid congestion, the bond length values are given only for three decimal places (Table 2).

The (aaa)-BNNN and (eee)-BNNN conformers have three symmetry planes along the axes of the needle, while the (aea)-BNNN and (eae)-BNNN conformers have just one symmetry plane, illustrated by the bond lengths presented in Figs. 4 and 5 where the 6 layer conformers are shown, as examples (see comments at Table 1).

The features of the bonding patterns in terms of bond lengths are in good agreement with the calculated molecular isoelectronic countours (MIDCO's). In Fig. 6 (part I) MIDCO's are shown for the (aaa) conformer for the $n = 6$ number of layers at various isodensity values. At the 0.16 a.u. isodensity value, the electron density appears as a continuous, connected, and single density domain. At higher isodensity value, 0.19 a.u., the electron density

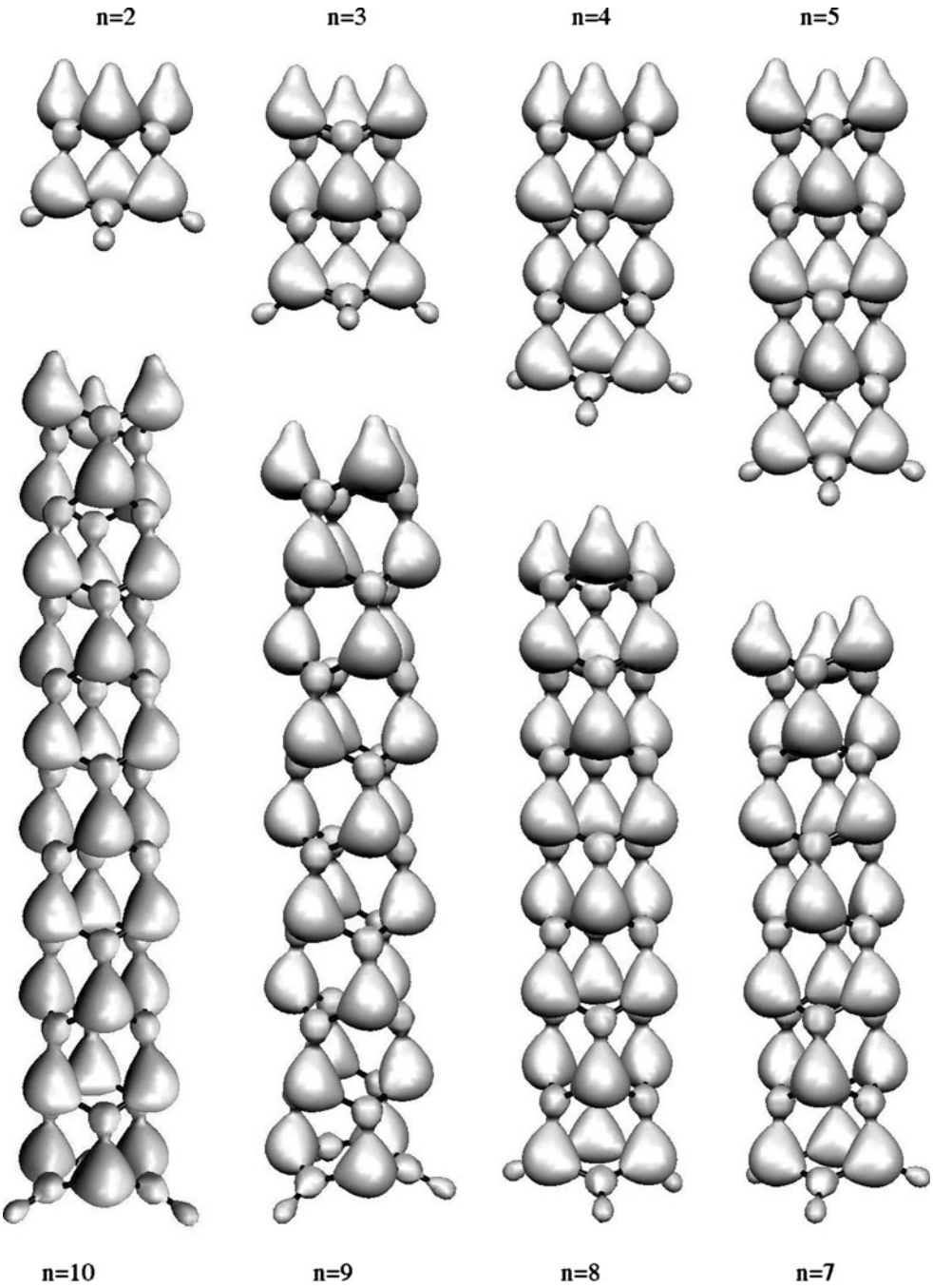

Fig. 7 Isodensity contours of 2, 3, 4, 5, 7, 8, 9, 10 layer—(aaa)-boron/nitrogen nanoneedles at 0.19 a.u

appears as connected just between some of those nuclei which form the bonds along the axis of the molecule, but there are no connections along the weaker in-layer bonds. Increasing the isodensity value further around each nucleus eventually, one finds an individual density contour.

The atomic and bonding ranges of the electron density can be also observed for (eee) (aea) (eae) $H_3(B_3N_3)_6H_3$ conformers shown in Fig. 6 (part II), where the isodensity contour is shown in gray, while the formal lines symbolizing bonds are black. A series of isodensity contours of (aaa) $H_3(B_3N_3)_nH_3$, $n = 2, 3, 4, 5, 7, 8, 9, 10$ are shown in Fig. 7, at the 0.19 a.u. threshold value. This choice of the threshold of 0.19 a.u. for the purpose of illustrating the results is motivated by the actual disconnection of some density domains at this value, showing separate electron density ranges, making the differences in some of the bonds evident. The visual illustration of the results provides a direct impression of the role the lone pairs play at the N-terminal, with the bulky equatorial lone-pair arrangement (for axial NH bonds) and the direction-enhanced axial lone-pair arrangement for equatorial NH bonds.

Whereas the systematic "tapered" changes in the bond length between layers already suggest a systematic variation of rigidity along these nanoneedles, nevertheless, the interactions between molecular fragments are not restricted to the actual bonds between layers, and all such interactions contribute to rigidity. In fact, as it also follows from the "Holographic Electron Density Theorem" [41], there exist non-negligible interactions between neighbor, second neighbor, and even more remote layers as well, specifically, interactions between layers which are not neighbors also contribute to local properties, such as bond lengths. Consequently, it is informative to test directly the effects of actual deformations on the molecular total energy; rigidity, in fact, can be evaluated based on the energy changes required for a given deformation.

For these reasons, the optimum structure of the aea—$H_3(B_3N_3)_6H_3$ conformer taken as a reference, the interlayer distances were systematically modified, stretched, as well as shortened by 0.02 Angstrom, and for these deformed structures, new energy calculations were carried out at the same level of theory. Since the sizes of deformations were the same for all these structures, the relative energy changes provide direct indications for the relative rigidities against each of these deformations.

The results are summarized in Table 3. Since interactions are not restricted to those bonds which were stretched or shortened, for valid comparisons one should take into account, at least in some approximate way, the changes of non-bonded interactions in the course of these deformations. Since in these needles the layer size molecular pieces are roughly comparable, it appears meaningful to compare deformations where on the two sides of the modified interlayer bonds the molecular pieces are of comparable size. For example, when the layer 1–layer 2 distance is modified, this is comparable with the case where the layer 5–layer 6 distance is modified, since in both cases the distance between a single layer piece and a five layer piece is modified, and similar non-bonded interactions are expected between pairs of molecular parts of comparable sizes. This is especially reasonable to assume, if the molecular pieces show a formal periodicity, as in our case. Similarly, when the layer 2–layer 3 distance is modified, this is comparable with the case where the layer 4–layer 5 distance is modified, since in both cases the distance between a double layer piece and a four layer piece is modified; again, similar non-bonded interactions are expected between pairs of molecular parts of comparable sizes.

Table 3 Relative energies (kJ/mol) of deformed aea—$H_3(B_3N_3)_6H_3$ conformer after stretching or shrinking the original distances between the consecutive layers by +0.02Å or −0.02Å, respectively; energy changes are relative to the conformer of the original bond length

Relative energies (kJ/mol) for deformed aea—$H_3(B_3N_3)_6H_3$ conformers		
N–H end = Layer 1	Bond length change orig + 0.02 Å	Bond length change orig − 0.02 Å
Layer 1–2	2.0229	2.0825
Layer 2–3	2.1721	2.2346
Layer 3–4	2.1674	2.2543
Layer 4–5	2.1786	2.2839
Layer 5–6	2.0634	2.2091

Energy change needed for a given deformation is indication of rigidity

Indeed, as seen in Table 3, the results show that for these comparable cases, the rigidity (as measured by the energy increase needed for the given 0.02 Angstrom deformation) is greater for deformations closer to the B–H end of the needle (where the interlayer bond lengths of the geometry-optimized structure are indeed shorter), as compared to the corresponding deformation closer to the N–H end of the needle (where the interlayer bond lengths of the geometry-optimized structure are indeed longer). Consequently, when the deformation involves molecular pieces of comparable sizes and structures, then the differences of bond lengths can, indeed, be taken as indications of relative rigidity. In such cases, a shorter bond length does indicate greater rigidity. Apparently, the fact that for such nanoneedles the rigidity is greater near the B–H end of the needles than near the N–H end can provide potential options for calibrating rigidity and flexibility if analogous nanoneedles become building blocks, such as spacer rods, in larger nanostructures.

4 Conclusion

Slight, but systematic deviations from perfect periodicity have been studied for narrow, rod-like polymeric structures. Electronic and structural properties of a series of boron/nitrogen nanoneedles have been discussed based on quantum mechanical computational methods. Four conformations of each molecule, (eee), (aaa), (aea), and (eae)-BNNN, have been found to have energy minima with no imaginary vibrational frequencies. Boron/nitrogen nanoneedles in analogy with similar carbon nanoneedles [40] are feasible, stable structures with interesting bonding features. The greater strength of the bonds along the needles, as compared to bond strength across the needles indicate considerable rigidity of such rods, nevertheless, this rigidity is "tapered": the bond length showing monotonic changes as one moves from the B–H end toward the N–H ends of these nanoneedles. Actual deformations, locally stretching or shrinking these needles between various layers indicate that the two ends show markedly different rigidity. Moving inward layer by layer from the two ends, the rigidity is always higher at locations closer to the B–H end of the needles, when compared to the corresponding layer closer to the N–H end. These systematic changes of bonding pattern and rigidity along the rods may have useful applications in potential nano-devices. This study showed that very long "infinite-length" BN nanoneedles are plausible, containing B_3N_3 unit cells. Such nanoneedles may serve as spacing rods and as potential building blocks in nanotechnology. The electron density analysis proved to be in good agreement with the pattern of bond lengths calculated for each structure, and support the interpretation of relative bond strengths along and across these needles, as well as the special importance of the N lone pairs.

Fortunately, the bonding systems in these structures are rather simple, and they apparently do not exhibit any of the complications where the actually applied DFT methodology is known to perform less than satisfactorily, such as cases of molecular instability, diradicals, possibly with unusual spin densities. Such features would make the results suspect and would make far more sophisticated methodologies necessary, nevertheless, even in relatively simple situations like the ones studied here, it might be worthwhile to carry out further studies with more advanced methodologies. Several possible extensions of these studies are of potential interest, and we thank the referees for pointing out some of these. The known problems with the B3LYP approach concerning spin densities and other sensitive molecular properties have pointed to the crucial role of the exchange correlation functional in a study by Filatov and Cramer [42], and the solutions suggested there could benefit the study of BN nanoneedles as well. Alternative DFT approaches, such as the Long-range Corrected (LC) DFT approach [43] of Hirao and coworkers could provide highly reliable and detailed results, and novel, multi-reference coupled cluster techniques [44, 45] of Yamaguchi and coworkers could further enhance the reliability of similar findings in nanoneedles. The highly accurate O(N) method for delocalized systems of Aoki and coworkers [46] is a promising approach for extensions of the present work to cases of highly conjugated nanoneedles, and an orbital approach to electron transport through heterocyclic aromatic hydrocarbons, proposed by Li et al. [47] may also provide new techniques to extend the present investigations. In general, such extensions may provide a broader, more reliable basis for drawing conclusions about small geometrical detail, even in nanoneedles with less conventional bonding patterns than those studied here.

Studies on alternative deformations, such as bending or torsion of analogous structures may reveal further interesting trends and rules, and vibrational and Raman studies can provide additional valuable information. By further, deliberate modifications of periodicity, for example, by the involvement of hetero layers, one can also obtain valuable information, in addition to further potential varieties of nanoneedles for the purposes of nano-design. In a different context, reaction path studies for processes of potential synthetic approaches leading to such nanoneedles can be of interest.

Acknowledgments This study has been supported by the Natural Sciences and Engineering Research Council of Canada (NSERC), the Canada Research Chair (CRC), the Scientific Modeling and Simulation Laboratory (SMSL), and Memorial University of Newfoundland. We thank for the Atlantic Computational Excellence Network (ACEnet) Atlantic Division for computer resources.

References

1. Hoffmann R, Imamura A (1969) Biopolymers 7:207
2. Imamura A, Aoki Y, Maekawa K (1991) J Chem Phys 95:5419
3. Maekawa K, Imamura A (1993) J Chem Phys 98:7086
4. Aoki Y, Imamura A (1992) J Chem Phys 97:8432
5. Aoki Y, Suhai S, Imamura A (1994) J Chem Phys 101:10808
6. Mitani M, Imamura A (1994) J Chem Phys 101:7712
7. Ladik J, Imamura A, Aoki Y, Ruiz y Ruiz MB, Otto P (1999) J Mol Struct (Theochem) 491:49
8. Mezey PG (1987) Potential energy hypersurfaces. Elsevier, Amsterdam
9. Heidrich D (ed) (1995) The reaction path in chemistry: current approaches and perspectives. Kluwer, Dordrecht
10. Mezey PG (1993) Shape in chemistry, an introduction to molecular shape and topology. VCH, New York
11. Rubio A, Corkill JL, Cohen ML (1994) Phys Rev B 49:5081–5084
12. Zunger A (1974) J Phys C-Solid State Phys 7:76–95
13. Zunger A (1974) J Phys C-Solid State Phys 7:96–106
14. Hoffman R (1964) J Chem Phys 40:2474–2480
15. Cusachs LC, Reynolds JW (1965) J Chem Phys 43:S160

16. Pople JA, Beveridge DL (1970) Approximate MO theory. McGraw Hill, NY
17. Lam PK, Wentzcovitch RM, Cohen ML (1990) Mater Sci Forum 54–55:165–192
18. Blase X, Rubio A, Louie SG, Cohen ML (1994) Europhys Lett 28:335–340
19. Johnson CJ, Zoellner RW (2009) J Mol Struct THEOCHEM 893:9–16
20. Czerw R, Webster S, Carroll DL, Vieira SMC, Birkett PR, Rego CA, Roth S (2003) Appl Phys Lett 83:1617–1619
21. Fuentes GG, Borowiak-Palen E, Pichler T, Liu X, Graff A, Behr G, Kalenczuk RJ, Knupfer M, Fink J (2003) Phys Rev B 67:035429
22. Lee RS, Gavillet J, de la Chapelle ML, Loiseau A, Cochon JL, Pigache D, Thibault J, Willaime F (2001) Phys Rev B 64:121405
23. Demczyk BG, Cumings J, Zettl A, Ritchie RO (2001) Appl Phys Lett 78:2772–2774
24. Chopra NG, Luyken RJ, Cherrey K, Crespi VH, Cohen ML, Louie SG, Zettl A (1995) Science 269:966–967
25. Loiseau A, Willaime F, Demoncy N, Hug G, Pascard H (1996) Phys Rev Lett 76:4737–4740
26. Lauret JS, Arenal R, Ducastelle F, Loiseau A, Cau M, Attal-Tretout B, Rosencher E, Goux-Capes L (2005) Phys Rev Lett 94:037405
27. Jaffrennou P, Barjon J, Lauret JS, Maguer A, Golberg D, Attal-Tretout B, Ducastelle F (2007) Loiseau A Physica Status Solidi 244:4147–4151
28. Marinopoulos AG, Wirtz L, Marini A, Olevano V, Rubio A, Reining L (2004) Appl Phys A Mater Sci Process 78:1157–1167
29. Man-Fai Ng, Zhang RQ (2004) Phys Rev B 69:115417
30. Wang JL, Mezey PG (2006) J Chem Inf Model 46:801–807
31. Wang JL, Mezey PG (2006) J Chem Inf Model 46:1965–1971
32. Szakacs CE, Mezey PG (2008) J Phys Chem A 112:2477–2481
33. Szakacs CE, Mezey PG (2008) J Phys Chem A 112:6783–6787
34. Szakacs CE, Mezey PG (2009) J Phys Chem A 113:5157–5159
35. Frisch MJ, Trucks GW, Schlegel HB, Scuseria GE, Robb MA, Cheeseman JR, Montgomery Jr JA, Vreven T, Kudin KN, Burant JC et al. (2004) Gaussian, Inc., Wallingford
36. Flükiger P, Lüthi HP, Portmann S, Weber J (2000) Swiss National Supercomputing Centre CSCS Manno Switzerland
37. Timoshkin AY, Schaefer HF III (2004) J Am Chem Soc 126:12141–12154
38. Timoshkin AY, Schaefer HF III (2008) J Phys Chem C 112:13816–13836
39. Kormos BL, Jegier JA, Ewbank PC, Pernisz U, Young VG Jr, Cramer CJ, Gladfelter WL (2005) J Am Chem Soc 127:1493–1503
40. Kormos BL, Cramer CJ, Gladfelter WL (2006) J Phys Chem A 110:494–502
41. Mezey PG (1999) Mol Phys 96:169–178
42. Filatov M, Cramer CJ (2005) J Chem Phys 123:124101–124107
43. Song JW, Tsuneda T, Sato T, Hirao K (2011) Theor Chem Acc 130:851–857
44. Saito T, Nishihara S, Yamanaka S, Kitagawa Y, Kawakami T, Yamada S, Isobe H, Okumura M, Yamaguchi K (2011) Theor Chem Acc 130:739–748
45. Saito T, Nishihara S, Yamanaka S, Kitagawa Y, Kawakami T, Yamada S, Isobe H, Okumura M, Yamaguchi K (2011) Theor Chem Acc 130:749–763
46. Aoki Y, Loboda O, Liu K, Makowski MA, Gu FL (2011) Theor Chem Acc 130:595–608
47. Li X, Staykov A, Yoshizawa K (2011) Theor Chem Acc 130:765–774